

This document contains classified information affecting the National Defense of the United States within the meaning of the Espionage Act, USC 50:81 and 32. Its transmission or the revelation of its contents in any manner to an unauthorized person is prohibited by law. Information so classified may be imparted only to persons in the military and naval Services of the United States, appropriate civilian officers and employees of the Federal Government who have a legitimate interest therein, and to United States citizens of known loyalty and discretion who of necessity must be informed thereof.

CLASSIFICATION CANCELLED

DEC 10 1940
RESTRICTED

TECHNICAL NOTES

NATIONAL ADVISORY COMMITTEE FOR AERONAUTICS

No. 786

STRUCTURAL TESTS OF A STAINLESS STEEL WING PANEL

BY HYDROSTATIC LOADING

By Ralph H. Upson
Stout Skycraft Corporation

to be returned to
the files of the Langley
Memorial Aeronautical
Laboratory.

Washington
November 1940



3 1176 01433 7571

NATIONAL ADVISORY COMMITTEE FOR AERONAUTICS

TECHNICAL NOTE NO. 786

STRUCTURAL TESTS OF A STAINLESS STEEL WING PANEL
BY HYDROSTATIC LOADING

By Ralph H. Upson

SUMMARY

A simplified type of all-metal wing construction of 18-8, spot-welded except for the skin attachment, was tested by means of hydrostatic loading, the wing being proportioned to permit close representation of typical conditions by means of the waterhead.

The general principle of design was to apply the skin on the wing under controlled initial tension and to utilize a finite internal pressure in flight. The initial tensioning was found to be an essential factor and the internal pressure in flight an important factor, although neither was critical with respect to small variations.

The results showed the possibility of eliminating almost all of the stiffeners from a stressed-skin wing, the possible reduction of weight in a lightly loaded wing and of substantial cost in the construction of any all-metal wing. Further experiments are suggested, however, on the magnitude and the effect of slight surface irregularities and on the contribution of the complete wing tip. A discussion of these suggested experiments is not included in the present paper.

With certain recommended improvements, the test method described is believed to be a valuable one for research on any new type of wing construction, particularly in cases where the covering, regardless of material or arrangement, is questionable.

INTRODUCTION

From formulas developed in reference 1, it can be shown that a fabric wing (fig. 1) is lighter than a metal-covered wing of prevailing construction (fig. 2) only by

the weight of the material required to handle the local pressure loads and to transmit them to the primary beam structure. Although this conclusion as to the source of the weight difference might be regarded as merely confirming common knowledge, the reason for the condition is not established since most of the weight, strength, and stiffness criterions for the materials themselves favor the metal rather than the doped fabric.

As might be expected, the discrepancy between theory and present practice is especially notable for lightly loaded wings and for a dense material, like steel. In this case the supposed necessity of closely spaced stiffeners or corrugations not only increases the weight but presents a serious cost problem.

The primary object of the tests described herein is to show the possibilities that may exist for an all-metal wing with even fewer parts than a fabric wing. If the arrangement is simple enough, metal can compare directly with fabric both in weight and in cost, and at the same time will provide well-known advantages of metals: stiffness, durability, resistance to fire, and general integrity of form and structure. Figure 3 shows the arrangement of parts in the wing panel built to test the possibilities mentioned.

Because the problem directly involves local pressures and strains in relatively large, unsupported skin panels, it was necessary to develop a method of testing that would set up these forces and reactions in their true relationship without the interference and uncertainty involved in shot bags or load pads. It seemed important also to consider the effect of variable internal pressure, at least between the limits of zero (atmospheric) pressure and maximum dynamic pressure q .

Preliminary analysis showed that the desired flight conditions can be closely simulated by making the wing watertight, mounting it in an inverted position, and filling it with water. With the proper waterhead and inclination, aerodynamic load distribution is then approximated, any desired internal pressure superimposed, and additional loads applied to a beam extension and to a torque arm attached for the purpose.

If well-known principles of structural models are used, such as have been applied to research on airship

hulls (reference 2), it is possible to test hydrostatically the structure of almost any wing. This statement is subject to the qualification, however, that when confined to the use of water for the load element the model will in many cases be larger than the full-size wing. For the present tests, conditions are selected that will make the scale factor unity; such conditions are met by a lightly loaded wing in which the proposed type of structure will show the greatest advantage.

It is believed, however, that both the type of structure and the test method can be used advantageously for higher wing loadings and other materials, particularly with respect to reducing production cost.

WING CHARACTERISTICS

General Proportions

The desired relationship between the aerodynamic and hydrostatic test pressure at the top of any wing is approximately attained under conditions of operation that make the pressure difference, in pounds per square foot, across the maximum section, numerically equal to 62.4 times the thickness of the wing in feet. The equivalent hydrostatic unit-spanwise loading is equal to 62.4 times the section area in square feet plus twice the unit wing weight, per unit local span. It then remains to assume such airplane characteristics that the foregoing conditions will be satisfied for a speed, loading, etc., that will be of practical interest.

The aerodynamic and hydrostatic pressure distributions are most closely comparable for an airfoil with a well-rounded top surface in combination with a nearly flat bottom. For this reason, and to take advantage of existing aerodynamic pressure data (reference 3), the NACA 4400-series airfoil was used, except that the camber line was slightly modified behind the 40-percent point. For points behind 40-percent chord, the camber-line equation:

$$\text{camber ordinate (percent chord)} = 4 - \frac{(x - 40)^2}{400} + \frac{(x - 40)^{5/2}}{5580}$$

where x is the abscissa in percent of chord behind the leading edge.

This change avoids the discontinuity in curvature otherwise existing at the 40-percent point; it permits a more straightforward skin-stress analysis, the other characteristics being only slightly affected.

The plan form is shown in figure 4. Outboard of the test panel root the wing is assumed to be straight tapered on a straight 0.30c line. A typical section at the center (volume center of middle skin panel) has 44 inches nominal chord, 6.75 inches (15.35 percent) thickness, and the top skin radius is 40 inches at 0.30c. The terms top and bottom will refer to the wing in its normal flying position.

The areas listed include a flap extending from 90 percent to 110 percent of the basic chord c . The actual test section terminates with the flap hinge line at 0.90c, the rear spar web being at 0.86c, which makes the water-filled plan-form area 18.45 square feet. Except for the flaps-down condition, the extended trailing edge is assumed to be in a neutral position with respect to the basic airfoil section. Moment coefficients are given in terms of the basic chord c .

Structural Design

Stainless steel 18-8 was used throughout the structure, the frame being spot-welded (fig. 5). The skin of the same material was 0.005 inch, half hard, screwed to the ribs with shakeproof no. 4-40 screws spaced 1/2 inch apart and with no stiffeners except one at the extreme leading edge. The single-beam web was at 0.30c, the flanges extending forward and unattached to the skin. The flap spar was at 0.86c to 0.90c. The unit weight was 1.5 pounds per square foot and designed to carry 10.7 pounds per square foot wing loading.

In order to provide an internal structure consistent with the 24-inch skin width, a rib spacing of 23-1/2 inches was used, braced in the top surface by diagonal members in a direction to take compression due to negative torque and drag loads. (The diagonals were later removed.)

The rib-flange elements were of 3/8-by-1/2-by-0.020-inch angle section full hard. These angles were bent by crimping, and cross-braced by hat lattices. The diagonals were of the same hat section, with the skin across the open face.

In figures 3 and 5 the basic simplicity of the structure is readily apparent. The structure involves but few parts and a small fraction of the amount of welding hitherto thought necessary in a stainless steel wing. Although it seemed possible that this simplification had been carried too far, it was desirable to lean in the direction of over-simplification for an experimental structure in order to establish safe limits for practical use later.

The test panel was made substantially watertight by the use of a standard caulking compound. An actual wing will be vented to the air to the extent required for any wing of similar size and performance characteristics. The vents, however, will be segregated in positions that will give a range of pressure for different conditions best suited to the structural effect desired. The representation of such pressures in the test panel will be made more clear in the description of the means for producing them hydrostatically.

The end bulkheads were of solid steel plate, stiffened around the edges, with the necessary mounting attachments and water connections. Beam and torque arms were carried at the outer end for the application of additional load.

Skin Tests and Attachment

Tests on skin samples, 0.0050 to 0.0052 inch half hard, showed the same ultimate tensile strength in both directions: 145,000 pounds per square inch or 750 pounds per inch. A screwed sample, with the designed seam proportions, tested in tension across the grain of the sheet, had substantial yield at 140 pounds per screw and failed at 150 pounds per screw or 300 pounds per inch of seam.

For skin application, the test panel with the skin on but not joined was mounted right-side-up with the basic chord horizontal. An upward load of 360 pounds was put on the beam arm extension at 0.30c and 109 inches out from the panel center, equivalent to a load factor of 1.90 in the wing-beam flanges. As this loading resulted in a substantial positive twist, the tip trailing edge was jacked up with a force of 64 pounds, sufficient to reduce the twist to 0.0035 radian and to increase the load factor to 2.04. After an interval of 16 hours, with the same beam load, no appreciable change was observed in the beam or torque deflection but the trailing-edge force had dropped to 55

pounds. The position was then fixed by blocking up the beam arm, and the top skin was joined, with the beam flange load factor approximately 1.6 at the root, 2.0 at the panel center, and 2.7 at the tip; the corresponding shear load factors were 0.8, 1.2, and 1.8, respectively.

After the top skin was attached, the panel was inverted, 40 pounds of torque arm and beam reinforcing weight were removed, and a jack force of 200 pounds was applied at the center of the beam arm extension at 30 percent chord and at 78 inches from the panel center. With the test panel thus loaded, the bottom skin was joined.

The final weights and their moments are listed in table I.

Required Loads

The requirements and notation from references 4 and 5 are employed in the following outline of flight conditions.

Condition I of the CAA which is critical for the wing beam, at a maximum dynamic pressure $q = 36.9$, makes the load factor $n = 4.67$; $C_n = 1.35$; $C_c = -0.29$ (perpendicular to the spar web); and $C_M = -0.08$ about the aerodynamic center at 25 percent of the basic mean aerodynamic chord.

Condition III giving maximum wing torque, at $q = 78.4$, makes $n = 3.20$; $C_n = 0.44$; $C_c = 0$; and $C_M = -0.08$ about the same aerodynamic center.

Condition VII with 30° flaps at $q = 25.6$, makes $n = 2.00$; $C_n = 0.84$; $C_c = 0.14$; and $C_M = -0.15$ about the same aerodynamic center. With conventional construction this condition would be less critical in torque than condition III, but because of the lower available pressure difference on the skin the tendency of condition VII to shear wrinkles may be increased.

For the given wing proportions (table II) and a slight center section cut-out, it is safe to assume that the span is loaded uniformly in proportion to the chord. For present purposes the wing weight is assumed to be similarly distributed.

With a wing loading of 10.7 pounds per square foot and a wing weight of 1.5 pounds per square foot, the net effective loading (for span distribution) is $9.2n$ pounds per square foot, where n is the load factor. If this loading is applied as a factor to columns 4 and 5 in table II, it gives the total shear and bending moment, respectively. Thus, the static root moment is 29,200 inch-pounds, which for an effective beam depth of 7.11 inches gives a flange force of 4100 pounds. The total static shear at the panel root is 412 pounds. With an included angle between the beam flanges of 0.0325 radian, the shear carried by the beam web is reduced by 4100 pounds times $0.0325 = 133$ pounds, and a net web shear of 279 pounds remains (if it is assumed that none is carried around the leading edge and the trailing edge).

In a similar manner, the required torque on any section equals the figure in the last column of table II multiplied by $0.107 n(x - 25) + C_m q + 0.015 n(40 - x)$ where x is the point (in percent chord) about which the torque is desired, C_m is the moment coefficient about the quarter chord, and q is the dynamic pressure. The last term approximates the effect of the wing weight, its center of gravity being assumed at $0.40c$.

WING PANEL TESTS

Test Conditions

The method of mounting is shown in figure 6. At the panel center (see table II), where most of the test data were taken, the static flange force and the net web shear are 2850 pounds and 207 pounds, respectively. Since the section area of the upper beam flange at this point is 0.264 square inch, its static stress is 10,800 pounds per square inch. This stress value tentatively neglects secondary stresses due to skin tension and beam stresses carried by the leading edge and the rear spar. Multiplying by the load factor gives the actual stress.

Integration of the water-filled section between the leading edge and $0.86c$ gives a section area of $A = 0.66cz_{\max}$ at a center-of-gravity position $\bar{x} = 0.40c$ back of the leading edge, where z_{\max} is the maximum section depth (fig. 7 and table II).

The water pressure = 0.036 pound per square inch per inch of head. The maximum pressure (maximum suction over top of wing) is approximately $p_m = 0.20 + 0.036H + 1.00 \alpha$ where H is head (inches) above the wing bottom at 0.86c on the panel center and α is the angle in radians between the chord and a horizontal plane.

Figure 8 shows the aerodynamic and the hydrostatic pressure variation over a section through the center. The water-filled portion is 72 inches long, or 3/4 inch more than the nominal panel length at each end.

For the added load required to represent flight conditions, the beam weight and its arm could be proportioned to give the correct combination of shear, bending moment, and torque at the panel center. Although this procedure gives a reasonable weight and length for the beam arm at the lower load factor of 1.6, it involves an inconveniently large weight and short arm at the higher factors. Actually, a variable weight was used on a constant beam arm and part of it was shifted over a constant torque arm to give the desired beam and torque moments. This compromise loading makes the shear lower than its correct value at the higher load factors and is valid only under conditions for which the beam shear is not critical.

The tests were based mainly on condition III of the CAA ($C_L = 0.48$) with load factors varied by varying q , typical values being listed in table III. The last load condition in the table represents condition VII (with flaps) for a load factor up to the full limit of 2.0.

For the coordination of experimental results with theory, the initial radius of skin curvature is an important parameter. This curvature has been computed at the panel center, for the modified 4400 series airfoil as described in a previous section, the results being plotted in figure 7, together with section areas for use in torque computations.

A large part of the underlying theory has been developed and is outlined in the appendix.

Observations without Water

The most conspicuous inequalities in the skin, after completion of the test panel but before it was filled with

water, were tension wrinkles in the bottom radiating from the tip end of the beam flange. These wrinkles were spread out but not eliminated by installing two supplementary tension straps from the beam arm to the panel tip. The same condition was accentuated in the case of the water-loaded wing at low internal pressure, as shown in figure 9.

A hollow, loose spot above the leading edge in the root skin panel and a slight one in the center panel were evidently due to the attachment of the skin to a straight leading-edge stiffener and the subsequent deflection into a curve during attachment to the ribs.

Small wrinkles in the top skin at the root end of the beam flange coincided with the point at which the section thickness had been increased to carry the skin over base plates in the mounting structure.

Other slight local puckers were visible along seam lines, particularly at rib 2 near the wing beam and the trailing-edge spar. The seams in general were somewhat wavy, apparently because of deposits of the caulking compound between the screws.

As an experiment to test the sound-deadening qualities of an asphaltum preparation advocated by its manufacturers, some of this compound was sprayed on the inside of the bottom on the middle and tip panels. In comparison with the untreated root panel, the effect was clearly appreciable, but it was believed that the difference was not worth the average increase in weight of 0.1 pound per square foot that would be involved. It appears possible, however, that a more effective distribution of the material might be found.

As shown in figure 6, the beam and torque strain measurements were taken at the ends of a transverse rod mounted across the tip at 70.5 inches from the root, with its front and rear ends 46 and 54 inches, respectively, from the beam web. The rod, 100 inches long, gave a reading of 0.01 radian twist for a 1-inch difference in height at the ends. The elastic or shear axis was established at the point at which there was no vertical deflection for a change of torque alone. Numerically, the beam deflection probably includes some deflection of the root bulkhead and mounting fixture.

Preliminary tests with no water showed that with the residual torque due to the panel and equipment weight, as listed in table I, the tip had a positive twist of 0.0102 radian. Increasing the beam moment (at the panel center) by 15,900 inch-pounds deflected the tip at the web 0.37 inch.

A superimposed couple of -1000 inch-pounds decreased the twist by 0.0031 radian around an elastic center slightly behind the web.

Hydrostatic Test Procedure

Unless otherwise stated, test data refer to the panel center (volume center of center skin panel). The load factor n is the bending moment at this point divided by the static bending moment.

For each condition listed in table III, α and H were chosen to give a pressure distribution over the top of the wing (on the chord section) as near as possible to the average difference between the prescribed internal pressure and the outside aerodynamic pressure. The angle α is measured in radians between the root basic chord and a horizontal plane, and H is the waterhead in inches above the wing bottom at 0.86c.

For the half-limit-load of condition III of the CAA the agreement between the aerodynamic and hydrostatic pressures is almost exact over the entire top of the wing section, as shown by the dotted curve at the top of figure 8. The comparisons of the two curves for the full limit of conditions III and VII are shown in the same figure.

The normal procedure was to apply the full required extra beam load, at the plane of the beam web and then to shift the load in 50-pound increments (equivalent to 1000 inch-pounds) out to the end of the 20-inch torque arm (fig. 6) to a total at least equal to the required torque load.

As the twist was a substantially linear function of torque in all cases, the results in table IV give the total twist (column 9) only for the one torque corresponding to the assigned condition of loading, with the rate of change in column 10.

Column 11 gives the approximate effective internal pressure in flight, as a proportion of the maximum dynamic pressure, and counting atmospheric pressure as zero.

Figure 10 shows the method used to locate the elastic center, which was approximately 4 inches behind the web for all conditions. It could not be determined more closely because of the small angles of twist and the difficulty of measuring deflections to within $1/32$ of an inch.

Results

The only permanent set observed in individual parts up to limit loading was due to the bow in the forward rib flanges under conditions of high pressure, which will be referred to later.

Under static load conditions ($n = 1$) there were no appreciable wrinkles in the top skin at any internal pressure from atmospheric to maximum dynamic pressure. The spanwise wrinkles in the bottom, however, were smoothed out only at pressures approaching maximum dynamic pressure (24.4 pounds per square foot). Bulging of the top skin was very noticeable under large bending moments combined with a large head of water. This bulging caused short wrinkles along the rib seams directed toward the center of each individual skin panel. (See figs. 11 and 12.) With a center bending moment of 28,600 inch-pounds (at half the limit-load factor of condition III), the top bulge was about $1/16$ inch, this deflection being nearly constant over most of the skin width between ribs (fig. 13). With the diagonals in place, these wrinkles along the ribs tended to slant in the direction of the diagonals, even against the effect of substantial applied torque, thus indicating a harmful effect of the diagonals.

With the diagonals cut, the slant of the rib wrinkles was reversed for moderate torque. The difference in twist with and without diagonals was so small that it could not be measured accurately. The wrinkles were definitely reduced at the 1.6 load factor and were just perceptible at about 1.3. Wrinkles were not visible completely across the top center panel until a torque of 4,000 inch-pounds was applied. This torque was 230 percent greater than required for the half-limit load of condition III. With 4,700 inch-pounds the wrinkles were

not much more pronounced. They occurred sooner in the root panel and later in the tip panel. A hysteresis effect caused the wrinkles to disappear at about 500 inch-pounds lower torque than that at which they formed (half-limit beam load of condition III at atmospheric pressure).

A distinct outward bow was noticed in the bottom rib flanges just forward of the beam when the head of water was large. This bow was caused by an abnormally high outward pressure. In actual flight, the bottom skin pressure (outward) is slightly negative for zero internal pressure. For the half-limit load of condition III the pressure at this point was -1.17 pounds per square foot, as fairly well represented by the water. For higher load factors, the bottom skin pressure would actually be a greater negative value. In order to approximate the average top skin pressures at the higher load factors, however, the bottom pressure was necessarily increased to a fictitiously high value.

After the completion of the tests recorded by table IV, the panel was drained and a check was made of the top skin tension by mounting the panel upright and observing the bending moment necessary to make the skin panel just slack. This bending moment was approximately 22,700 inch-pounds at the center, corresponding to $n = 1.54$ and a flange stress of 14,400 pounds per square inch, a 33-percent reduction from the bending moment used in applying the skin. This reduction is thought to be due mainly to creep at the screw holes in bearing.

A final test to destruction was made of the beam structure under condition I (fig. 14). Although tests of the internal structure were not included in the present project, it is of interest to note that buckling of the compression flange produced no failure or leakage in the skin.

DISCUSSION OF TEST METHOD

As might be expected from the first use of a new method, several improvements are indicated for future use of hydrostatic wing testing:

1. In order to avoid local seam irregularities, little if any caulking paste should be put within the seam lap. Final watertightness should be

obtained; in preference, by use of a liquid caulking compound applied from the outside. This method was tried locally with complete success.

2. Because of the small deflections to be measured, deflection gages capable of magnifying the readings about ten times should be used in preference to direct measurements. Strain gages for direct measurement of the skin strain proved to be neither feasible nor worth while.
3. Determination of surface waviness to a magnitude as low as 0.001 inch in 1 inch will apparently be an important consideration in future tests for correlation with air-flow experiments on the location of the transition point from laminar to turbulent flow. A suggested method of taking such measurements of the surface is by the use of a Tuckerman strain gage set at right angles to its usual position, to measure the vertical rise or depression between two other contact points. All contacts for this purpose must be very light.
4. As previously indicated, the use of water in the actual wing section is restricted by its density to relatively low wing loadings, speeds, and load factors. It appears possible, however, to extend greatly the practical application of the method by the use of heavier liquids. One suggestion is that with fine metallic particles or other particles in colloidal suspension (e.g., red lead paint) it may be possible to get a practical liquid with a specific gravity up to at least 3. Data on various miscible minerals possible for use in preparing liquids of high specific gravity are given in reference 6, page 109.
5. Especially in conjunction with the choice of liquids varying in specific gravity, it becomes desirable to apply the method to a complete half-wing, which will avoid the necessity for such substantial added loads and will show the requirements with respect to the tip structure.

The method of test is applicable to any type of wing construction, with either metal, wood, or fabric cover. In the case of fabric, for example, it furnishes a means for the quantitative study of fabric strength and tightness, rib spacing and structural arrangement, pressure effects, etc., that have hitherto been decidedly lacking in such design.

As the tests indicated, the question of how much the internal pressure should be dropped below maximum dynamic pressure must still be settled. The single stiffener used in the test panel proved ample for structural purposes even at pressures down to zero. At certain locations of the stagnation point, however, the application of outside pressure greater than the inside caused a slight elastic cupping of the skin between ribs. The aerodynamic effect of such deformation could be determined as part of a more general study of air flow conditions, preferably on a full-scale structural panel.

GENERAL CONCLUSIONS

The results indicate the general feasibility of a simplified all-metal construction in which very thin skin (in this case 0.005 inch) carries tension only, without stiffeners or diagonals and with a rib spacing of 2 feet. Static loads including torque were carried without visible wrinkling; wrinkling at higher load factors was almost entirely confined to the neighborhood of the edge attachments along the chord lines.

Initial stressing, particularly of the top skin in a spanwise direction, was beneficial and could undoubtedly be increased to advantage, especially toward the root. The spanwise tensioning of the lower skin should, if anything, be reduced in favor of a little chordwise tensioning in the flat portion. In order to allow for skin loosening when applying the skin and under flight conditions, the initial strain in the structure should be made at least 50 percent greater than the final strain difference that is desired. A stiff wing tip is shown to be of advantage.

Chordwise curvature, while helping to carry the load, encouraged edge wrinkles; hence, a better balance of structural proportions would require less curvature in the forward part of the wing except near the extreme leading edge where local stiffening can be retained.

Because of the large external suction over the top, internal pressure above atmospheric was found to be of but slight benefit on the top skin but tended to smooth out spanwise wrinkles in the bottom skin. Pressure as high as maximum dynamic pressure was definitely harmful in every case except for flap condition VII at a maximum speed of 100 miles per hour. The skin was not sensitive to small variations of pressure. Torque stiffness was greatest at the higher pressures.

For a wing approximating the design characteristics here shown, the best position of the air vents would appear to be in the bottom just forward of the flaps. This position would induce an internal pressure of $0.2q$ to $0.5q$ for normal operating conditions, the pressure would increase to $0.7q$ with flaps down 30° .

The wing, as designed for a wing loading of 10.7 pounds per square foot, was about 25 percent lighter than the conventional all-metal construction for the same loading (reference 1) and it saved 75 percent of the fastenings (spot welds or rivets) that would be used in an equivalent conventional construction. In stiffness, at zero pressure, the wing is 40 percent above the present GAA requirements (reference 5); with the suggested pressure control, it is nearly 80 percent above these requirements.

If the saving in fastenings, laps, and incidental irregularities is applied to current riveted construction, it is estimated from reference 7 that the parasite wing drag will be reduced about 12 percent for countersunk rivets and jogged laps or 25 percent for brazier-head rivets and plain laps.

On the other hand, from reference 8, a continuous wave 3 inches wide and 0.02 inch high at 10.5c on the upper surface will increase the drag 6 percent. Although the waviness under normal flight conditions was apparently of a small order of magnitude, the condition and its effects should be accurately determined by methods such as have been suggested.

Stout Skycraft Corporation,
Dearborn, Mich., October 4, 1940.

APPENDIX

EFFECTS OF PRESSURE AND STRAIN ON LARGE SKIN PANELS
OF THIN SHEET

General Balance of Forces

Any given skin panel is in equilibrium under the action of pressure forces distributed over its surface and of edge reactions distributed around its periphery. For present purposes it is assumed that the distribution of pressure (or, more properly, pressure difference between inside and outside of the skin) and the initial relationship between the various parts of the structure are known.

As a simple case in a complete surface of revolution, such as a metal airship hull (reference 9), the stress analysis is relatively determinate in the sense that the shape remains practically constant; hence, the skin stresses resulting from the pressure and from integrated shear and bending moment are direct reactions even if they are somewhat involved. In an airplane wing, however, the strain takes place in such a way as to produce a relatively large deflection which, in turn, is an important factor in the stress that produces the strain. This results in essential indeterminacy because: first, there are two principal directions of skin stress; secondly, initial stresses or those due to the wing bending moment cannot be superimposed on the skin in any direct way; and, finally, buckling in the direction of minimum stress again changes the test conditions to a different basis.

General analysis involves consideration of compressive and bending stresses in the skin as in reference 10. In the appendix of this reference, however, it was shown that skin panels of the proportions here used can, without substantial error, be considered as tension diaphragms with negligible flexural rigidity, except at the edges along the supports, where high local bending stresses may develop in certain cases. Hence, a simplified analysis is used in this paper, stiffness in bending being tentatively neglected and the direct compressive strength being considered zero except for the conventional effective widths adjacent to the supports.

Attention is at first confined to the case of uniform pressure on a single-curved skin, where all curvature is in the direction of the panel width and the straight elements are infinitely long. Based on an exact solution for this case, practical engineering formulas are developed for the skin stress and deflection that are due to the combination of tension and pressure over a given panel.

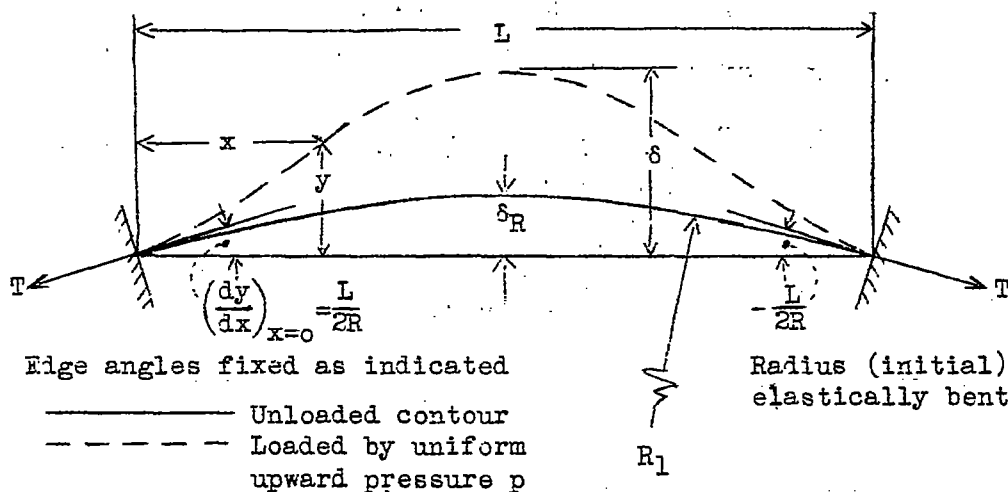
Strain in the supporting structure is tentatively assumed at the maximum allowable value for the most critical case and readjusted by trial and error for other cases.

The effect of initial curvature, stress, and strain in a direction at right angles to the panel width is approximated by considering it as equivalent to a change in the effective pressure. The corrected value for the panel deflection is then made the basis for final stresses due to all forces except shear.

Shear is handled by the usual method of principal stresses as long as the minimum stress does not become negative and reach a buckling value.

The non-uniformity of pressure and curvature is a serious problem only in cases where the variation is large along an important line of skin stress. For present purposes it is assumed that a mean effective value can be satisfactorily estimated.

Symbols and Initial Assumptions



The sketch shows a section across the skin panel in the general case for single-curved deflection of initially flat skin. All data relate to a 1-inch strip. The material is assumed elastic, homogeneous, isotropic, and of uniform thickness. The X-axis passes through the two points of support, one of which is taken as the origin. Tensile stress and moments producing concavity upward are considered positive.

The symbols used in the analysis are:

- p pressure on concave side minus pressure on convex side, assumed uniform and normal to skin surface, pounds per square inch
- p_n maximum outward pressure at top of wing
- p' net pressure carried by one component of skin tension
- h skin thickness, assumed small compared to L , inches
- E modulus of elasticity of material
- μ Poisson's ratio, assumed 0.3 in the report
- D flexural rigidity $\left(\frac{EI}{1 - \mu^2} \right)$ which for a 1-inch strip of uniform unstiffened skin equals $\left(\frac{E h^3}{10.9} \right)$, inch-pounds
- L skin width or rib spacing in spanwise direction, inches
- T tension in same direction, pounds per inch
- R radius of curvature at any given point, inches
- R_1 initial radius of skin, the center of curvature being defined by the intersection of the two normals erected at the two points of skin support.

l, t, r the respective items corresponding to L, T, R in a direction parallel to the wing chord

- e_L and e_t the respective unit initial skin strain in the same two directions due to all causes except extension of the skin itself under normal pressure
- e total unit strain in any one direction
- M bending moment in a 1-inch strip of skin at any point (x,y) , inch-pounds per inch
- M_e bending moment at edge, inch-pounds per inch
- δ maximum ordinate or final total deflection, inches (assumed small compared to L)

Relation between Deflection and Stress

For the previously mentioned condition of negligible flexural rigidity in two principal directions but no shear, the elementary balance of forces gives:

$$p = \frac{T}{R} + \frac{t}{r} \quad (1)$$

Assume that the initial radius in the span direction $R_1 = \infty$ and that r (in the chord direction) is practically constant and equal to the initial section radius r_1 ; the second term of equation (1) is most conveniently handled as a reduction of effective pressure. Thus the net pressure is written as:

$$p' = p - \frac{t}{r_1} = \frac{T}{R} = \frac{8 \delta T}{L^2} \quad (2)$$

For a small value of δ/L (parabolic arc)

$$\delta = \frac{p' L^2}{8 T} = \frac{L^2}{8 T} \left(p - \frac{t}{r_1} \right) \quad (3)$$

Assume that p' can be determined; a second equation is then required to solve for both T and δ . This equation is obtained from the strain relations.

The final skin strain in the L direction consists of three terms, the first one due to skin bulge and the other two due to the initial or the residual strain. Thus, if the Poisson effect is taken into account, the total unit strain in the skin is:

$$e = \frac{T(1 - \mu^2)}{E h} = K_g \frac{\delta^2}{L^2} + e_L + \mu e_t \quad (4)$$

where the geometric form constant $K_g = 8/3$ for the assumed parabolic arc; e_L and e_t are each the algebraic sum of the total unit strains in the supporting structure, under the conditions of loading, plus the residual difference in strain between the unbulged skin and the supporting structure.

If $\mu = 0.3$ and $K_g = 2.67$ are substituted in equation (4)

$$\delta = 0.613L \sqrt{\frac{0.91T}{E h} - e_L - 0.3 e_t} \quad (5)$$

which, with equation (3), permits the desired solution of δ and T if t can be determined. In the usual case in which t is not directly known, it can be considered to be made up of three terms:

1. Increment induced by the deflection δ . If complete local shear rigidity is assumed,* adding to r_1 is equivalent to extending l in the same proportion. As this extension applies only to the center element of the panel, a factor is applied based on the shape of the deflection curve for the mean effective tension over the panel as a whole. The slight change in R is here a second-order effect and can be neglected for a large value of l/L .

*The assumed shear rigidity means that sections cut by planes normal to the supporting edges before deflection remain in the same plane after deflection. The spacing of these planes may change, however, with strain in the supporting structure.

2. Increment induced by Poisson's ratio (from tension T in the L direction).
3. Portion due to relative elongation of the supporting frame in the l direction and/or the initial stretching of the skin (or thermal shrinkage) similar to that which has already been defined.

The sum of the three items gives, for $\mu = 0.3$,

$$t = \frac{K_t E h \delta}{r_1} + 0.3T + E h e_1 \quad (6)$$

where t is the average effective stress and K_t is a factor depending on the shape of the deflection curve. For a circular arc $K_t = 2/3$ and for a straightline $K_t = 1$. A combination of equations (6) and (3) for $K_t = 2/3$ gives:

$$\delta = \frac{1.5 r_1 L^2 (p r_1 - 0.3T - E h e_1)}{12 r_1^2 T + E h L^2} \quad (7)$$

The method of solution is to plot δ against varying T from both equations (5) and (7). The point of intersection of the two curves is then the correct value of δ and T .

Edge Moment in the Skin

Wherever the bending stress in the skin is appreciable, equation (1) must include terms due to the skin stiffness. By considering this stiffness effective in only the L direction, an adaptation of equation (2) expressed in differential form gives, by well-known principles, for small deflections:

$$p' = \frac{d^2 M}{dx^2} + \frac{T}{R} = D \frac{d^4 y}{dx^4} - T \frac{d^2 y}{dx^2} \quad (8)$$

which, for an edge moment of M_e , has the following general solution:

$$y = C_1 \sinh x \sqrt{\frac{T}{D}} + C_2 \cosh x \sqrt{\frac{T}{D}} + \frac{p' x (L-x)}{2T} - \frac{p' D}{T^2} - \frac{M_e}{T} \quad (9)$$

The integration constants C_1 and C_2 are determined in this case by putting the first derivative equal to zero at $x = 0$ and $x = L$, corresponding to initially flat spanwise elements. If the values thus obtained are substituted in equation (9), it can be solved for the edge moment, $x = 0$ and $y = 0$

$$M_c = \frac{p'L^2}{4} \left(\frac{2D^{\frac{1}{2}}}{LT^{\frac{1}{2}}} \coth \frac{LT^{\frac{1}{2}}}{2D^{\frac{1}{2}}} - \frac{4D}{TL^2} \right) \quad (10)$$

or for small values of $4D/TL^2$

$$M_c = \frac{p'LD^{\frac{1}{2}}}{2T^{\frac{1}{2}}} = \frac{p'L}{3.6} \sqrt{\frac{Eh^3}{T}} \quad (11)$$

For such conditions it can readily be shown by equation (9) that the skin stiffness is of negligible effect on the deflection. Hence, with p' expressed in terms of equation (3), equation (11) becomes

$$M_c = \frac{1.218}{L} \sqrt{Eh^3 T} \quad (12)$$

δ and T being both known from equations (5) and (8).

In using equation (12), it must be taken into account that fully elastic conditions are assumed; whereas, actually, plastic deformation will take place when the bending stress is high, thus altering the end condition in a direction to relieve the moment itself.

Shear Stress and Buckling

In reference 3 the attempt was made to evaluate the critical shear stress at which skin buckling takes place. Torque tests on an initially smooth panel showed, however, that it was practically impossible to identify the buckling point with any accuracy due apparently to the following causes:

The extreme edge tended to buckle first, and these wrinkles lengthened very gradually across the skin panel.

The wrinkling itself tended to take up slack in the material and to prevent any sudden increase of buckling.

As a result, the skin took far more than either the required or the theoretical critical shear without serious wrinkling as long as the skin was unbuckled under the given beam and pressure loads. Hence, the most important theoretical criterions seem to be the conditions that cause edge buckling along the rib attachments and those that cause the skin to slack in a spanwise direction. In order to avoid the buckling of the edge

$$0.3T + E\epsilon_1 > 0 \quad (13)$$

and to avoid spanwise slack

$$T > 0 \quad (14)$$

If $T = 0$ in equations (5) and (7) and if terms of a low order of magnitude are omitted, equation (14) can alternatively be expressed by the criterion:

$$\epsilon_L + 0.3\epsilon_1 > 0 \quad (15)$$

which is independent of pressure except as reflected in the relatively small second term.

With the assumed inability of the skin to take compression, equation (15) makes $T = 0$; then from equation (2), $t = p/r_1$ and a definite buckling occurs whether or not there is shear in the skin.

The unit initial skin strain, ϵ_1 is due to the stress in the rib flange, which for preliminary design purposes can be assumed at a given safe value and the rib can be designed to correspond. The actual force in the rib flange can be computed by the usual method, subject to an increment $-tL$ due to the skin tension.

If Δf_b is the beam flange stress (compression positive)* under which the skin is applied, f_{b1} is the final beam flange stress (tension positive) under static load, and n is the load factor,

$$\epsilon_L = \frac{\Delta f_b + n f_{b1}}{E} \quad (16)$$

*Considered as positive from a standpoint of skin tension.

$$\text{If } e_t \approx 0, \Delta f_b + n f_{b_1} > 0 \quad (17)$$

from equation (15), for preliminary analysis.

In other words, to avoid spanwise buckling of a surface with substantial convex curvature in the chord direction, it will usually be sufficient to apply the otherwise unstressed skin while the beam flange is stressed to correspond to the assigned loading, provided that the skin can be applied just taut and there is no creep in the material.

Example from Wing Panel as Tested, for Load Factor $n = 1.6$

In an analysis of the center skin panel on top of the wing, under water load, E (effective) can be taken at 26,000,000 pounds per square inch, and from data already given:

Rib spacing, $L = 23.5$ inches

Skin thickness, $h = 0.005$ inch

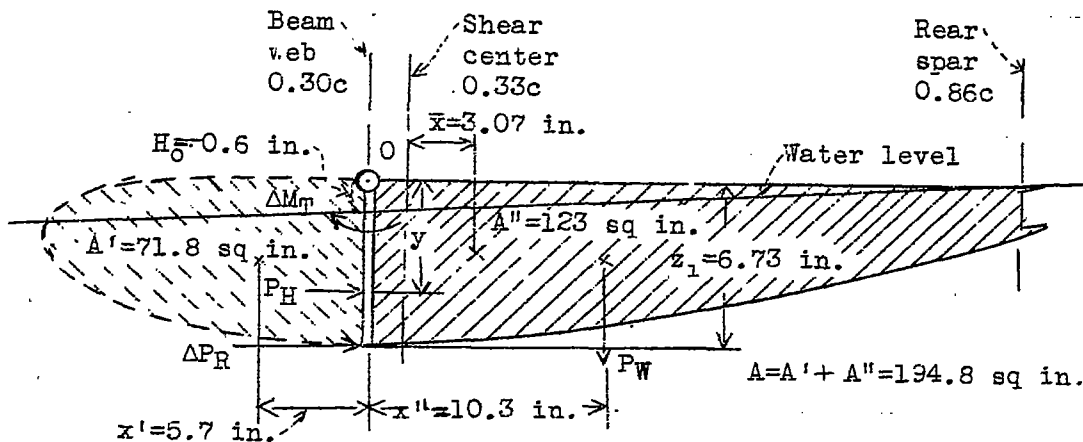
Surface radius, $r = 40$ inches

Beam stress, $f_{b_1} = 10,800$ pounds per square inch
(static)

Water density, 0.0361 pound per cubic inch

As already explained, the skin became slack at about $n = 1.34$.

This reduction from the assumed load factor of 1.6 made $\Delta f_b + n f_{b_1} = 10,800 (1.34 - 1.60)$ in equation (17); then $T = 0$ and $t = pr = 40p$. From the formula given under Test Conditions, for a waterhead $H = 0$ and $\alpha = 0.026$ (corresponding to atmospheric internal pressure), the pressure at the top of the wing (at 0.30c) is: $p_n = 0.200 + 0.025 = 0.225$ pound per square inch; and $t = 40p_n = 9.0$ pounds per inch. The increment of rib-flange force due to t is $Lt = 211$ pounds, to which must be added a net rib-flange force ΔP_R , due to pressure and torque reactions, to get the total force P_R .



From the sketch, the net rib-flange force $\Delta P_R = P_R - L_t$ just to the rear of 0.30c, is determined by putting its moment in equilibrium, about 0, with the moment due to the water weight: $P_W \bar{x}'' = 0.0361 L A'' \bar{x}''$, that due to the waterhead:

$$P_R y = 0.0361 L \left(\frac{H_0 z_1^2}{2} + \frac{z_1^3}{3} \right)$$

and the torque increment carried by the wing covering (taken as a couple):

$$\Delta M_T = -0.0361 L A \bar{x} A'' / A$$

where H_0 is the waterhead (inches) at point 0; A and $A \bar{x}$ are, respectively, the area and the first moment of area about the shear center, of the airfoil cross section; A' and $A' \bar{x}'$ are the area and the first moment of area, about 0 of the nose portion of the airfoil back to 0; A'' and $A'' \bar{x}''$ are the area and the first moment of area about 0 of the portion of the rib from 0 back to the rear spar; and z_1 is the depth of section at 0. These areas and arms are evaluated from figure 7.

The moment balance about 0 thus calculated may then be expressed as

$$\Delta P_R z_1 = 0.0361 L \left(\frac{-H_0 z_1^2}{2} - \frac{z_1^3}{3} + A'' \bar{x}'' + A'' \bar{x} \right)$$

from which the net flange force $\Delta P_R = 100$ pounds compression; to this force must be added an increment of 211 pounds due to skin tension, which makes a total rib flange force $P_R = 311$ pounds compression. The section area of rib flange $A_R = 0.025$ square inch. Then the rib stress is $f_R = -P_R/A_R = 12,400$ pounds per square inch, and $e_1 = f_R/E = -0.00048$, which is well below the value of $e_1 = 0$ already assumed in equation (15), thereby confirming the tentative value of $T = 0$ and the observed small wrinkles under the same conditions.

For a skin panel wrinkled into a general tension field, a modified type of analysis is required.

Discussion of Example

If these values of t and e_1 are used, and $K_t = 2/3$, in equation (6), $\delta = 0.039$ inch. This value compares with a measured deflection of 0.062 inch under equivalent conditions. It is believed that the small absolute difference is mainly due to vertical cantilever deflection, under load, of the front and rear portions of the ribs and to angularity of the marginal wrinkles. More complete measurements would be required to check this supposition.

The theory, without further correction, is apparently adequate to predict the conditions under which wrinkling will occur.

If it is assumed that all torque shear is carried in the skin and the trailing edge spar, the standard formulas for torque and twist give a torque shear in the skin of 510 pounds per square inch for a torque of 1000 inch-pounds. A computation for the corresponding twist gives 0.0015 radian in the panel length of 70.5 inches, which compares well with the observed values.

This agreement shows that the maximum twist in the water-loaded condition is still not appreciably greater than in the unwrinkled skin alone. Without water, the twist increment for the same torque was about double that of the mentioned value, which fits well the assumption that in such a case the skin shear is carried by tension in one diagonal only. Thus, under any practical flight load condition, the torque rigidity is substantially greater than would be apparent from conventional laboratory tests in which the skin would be free to buckle.

REFERENCES

1. Upson, Ralph H.: Performance Dictates Design. Jour. Aero. Sci., vol. 7, no. 9, July 1940, pp. 369-75.
2. Tuckerman, L. B.: Water Model Tests for Semirigid Airships. T.R. No. 211, NACA, 1925.
3. Pinkerton, R. M.: Calculated and Measured Pressure Distributions over the Midspan Section of the NACA 4412 Airfoil. T.R. No. 563, NACA, 1936.
4. U. S. Department of Commerce: Civil Air Regulations 04: Airplane Airworthiness, May 31, 1938.
5. U. S. Department of Commerce; Air Commerce Manual 04 Airplane Airworthiness, July 1, 1938.
6. Lange, N. A.: Handbook of Chemistry. Handbook Publishers, Inc., Sandusky, O., 1934.
7. Hood, Manley J.: The Effects of Some Common Surface Irregularities on Wing Drag. T.N. No. 695, NACA, 1939.
8. Hood, Manley J.: The Effects of Surface Waviness and of Rib Stitching on Wing Drag. T.N. No. 724, NACA, 1939.
9. Upson, R. H.: The General Problem of the Stressed-Skin Airship Hull. Airship Forum, Guggenheim Airship Inst., Akron, O., 1935.
10. Upson, R. H.: Arc Welding in Aircraft; Abridged reprint in Arc Welding in Design, Manufacture and Construction. The James F. Lincoln Arc Welding Foundation, Cleveland, O., 1939.

TABLE I.- FINAL PANEL WEIGHTS

Item	Weight (lb)	Weight beyond panel center	Span arm from center (in.)	Moment (in.-lb)	Chord arm from 0.3c (in.)	Torque (in.-lb)
Root bulkhead	79					
Wing panel	32	14	17	240	3.6	51
Tip bulkhead and braces	25	25	38	950	4.1	103
Load beam	75	75	76	5,700	-1.2	-90
Torque arm and clamps	17	17	105	1,780	8.0	136
Water	501 ^a	230 ^a	18.4	4,230	4.1	944
Total	729	361		12,900		1144

^aSubject to a small correction for skin bulge.

TABLE II.- WING DIMENSIONS

	Distance from root (in.)	Nominal chord c (in.)	Thickness ratio (percent c)	Effective beam depth (in.)	Area of overhang (sq ft)	Beam moment of overhang area (in.-sq ft)	Torque moment of overhang area ^b (in.-sq ft)
Root of test panel	0	49.96	15.77	7.11	44.85	3180	1700
Center ^a of test panel	34.85	44.00	15.35	6.00	32.35	1850	1110
Tip of test panel	70.50	37.89	14.72	4.83	21.15	890	650
Tip of wing	163.00	22.08	11.60	1.81	0	0	0

^aTaken at center of water volume of center skin panel where the maximum depth is 6.75 in., equivalent to 35 lb /sq ft of water pressure.

^bOverhang area multiplied by its nominal M.A.C.

TABLE III.- REQUIRED TEST LOADS FOR PROPER BENDING MOMENT AND TORQUE

Condition	Extra beam load ^a (lb)	Torque load ^b (lb)	Dynamic pressure q (lb/sq ft)	Angle of chord (radian)	Load factor	To be observed for:	Head H (in.) for atmospheric pressure
Static III	39	21	24.4	0	1.00	} Skin wrinkles	-1.3
Half-limit III	136	59	39.2	.026	1.60		0
Limit III	395	144	78.4	.078	3.20	Permanent set	3.0
Ultimate III	654	320	117.3	.130	4.80	Structural failure	6.0
Limit VII	324	100	25.6	.078	2.00	Wrinkles and permanent set	-1.3

^aAt point 69 in. out from panel tip (skin bulge and weight of beam arm tentatively neglected) 104.65 from panel center, at 0.3c except amount in next column.

^bOn 20-in. arm back of 0.3c; this weight included in first-column figures.

TABLE IV.- TEST RESULTS

1	3	4	5	6	7	2	8	9	10	11
Approximate GAA or other load condition	Basic root angle (radian)	Maximum pressure onto skin (lb/sq ft)	Bending moment ^a (1000 in.-lb)	Torque about 0.3c ^a (1000 in.-lb)	Normal shear ^a (lb)	Bending moment load factor	Deflection of tip relative to root (in.)	Twist of tip relative to root (radian)	Change in twist angle (radian per 1000 in.-lb change in torque)	Internal p/q (average over top)
Panel empty	0.026	--	8.7	0.20	131	0.51	0	0.0102	0.0031	--
Panel empty	.026	--	24.3	.20	280	1.43	.4	.0015	--	--
Panel empty	.130	--	8.7	.20	131	.51	0	.0114	--	--
Half-limit III	.026	32.2	28.6	2.14	510	1.68	.7	.0084	.0013	0
Half-limit III	.026	71.2	28.8	2.17	519	1.69	.7	.0087	.0011	1.0
Half-limit III	.078	78.5	30.0	2.17	530	1.76	1.1	.0086	.0011	1.0
Half-limit III ^b	.026	32.2	27.8	2.14	503	1.64	1.5	.0074	--	0
Limit III	.078	55.1	56.2	4.14	793	3.30	1.7	.0077	.0015	0
Limit III	.078	133.1	56.5	4.37	808	3.32	1.7	.0074	.0010	1.0
Ultimate ^b III	.130	78.0	83.6	5.57	1039	4.91	3.0	.0089	.0015	0
Ultimate III	.130	140.4	83.8	5.60	1048	4.93	2.7	.0090	--	.5
Ultimate ^b III	.130	140.4	83.8	5.60	1048	4.93	3.0	.0080	--	.5
Ultimate III	.130	78.0	83.6	5.57	1039	4.91	2.6	.0097	.0016	0
Limit VII	.078	32.8	35.1	3.14	593	2.07	1.4	.0067	.0016	0
Limit VII	.078	58.8	35.2	3.16	597	2.07	1.3	.0083	.0010	1.0
Limit VII ^b	.078	58.8	35.0	3.16	595	2.06	1.4	.0074	--	1.0

^aBending moment, torque, and shear refer to panel center.

^bNo diagonals between ribs; all other tests with diagonals.

Chord shear was calculated for all test conditions, but was critical for none. For ultimate loading of condition III, the maximum value was 189 lb.

"Tip" refers to tip of test panel.

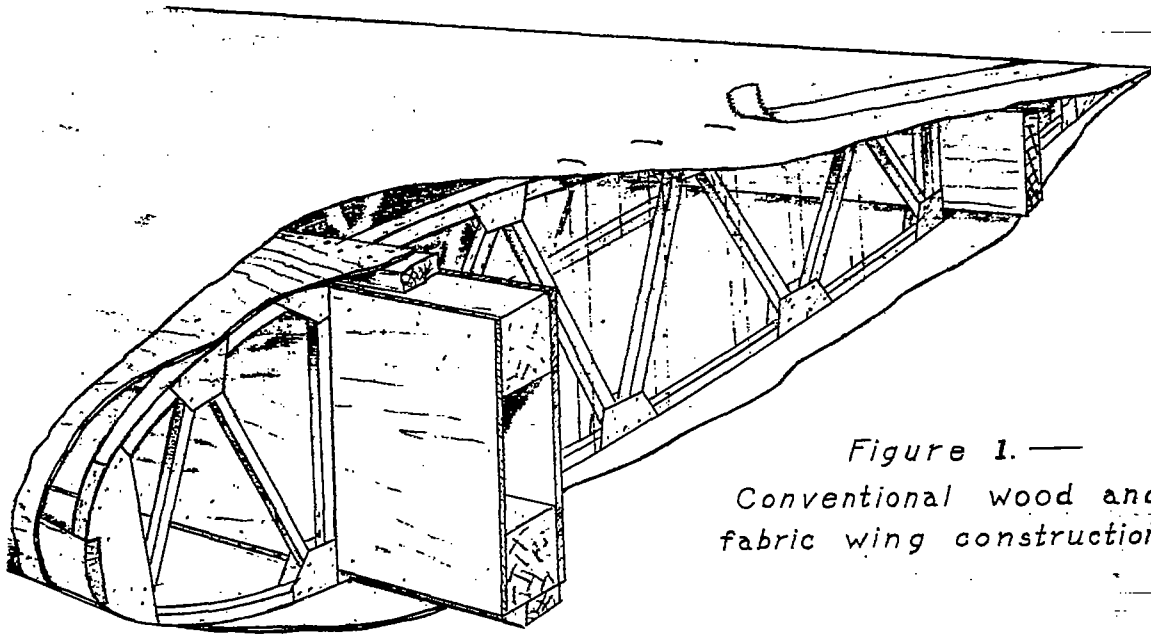


Figure 1. —
Conventional wood and
fabric wing construction.

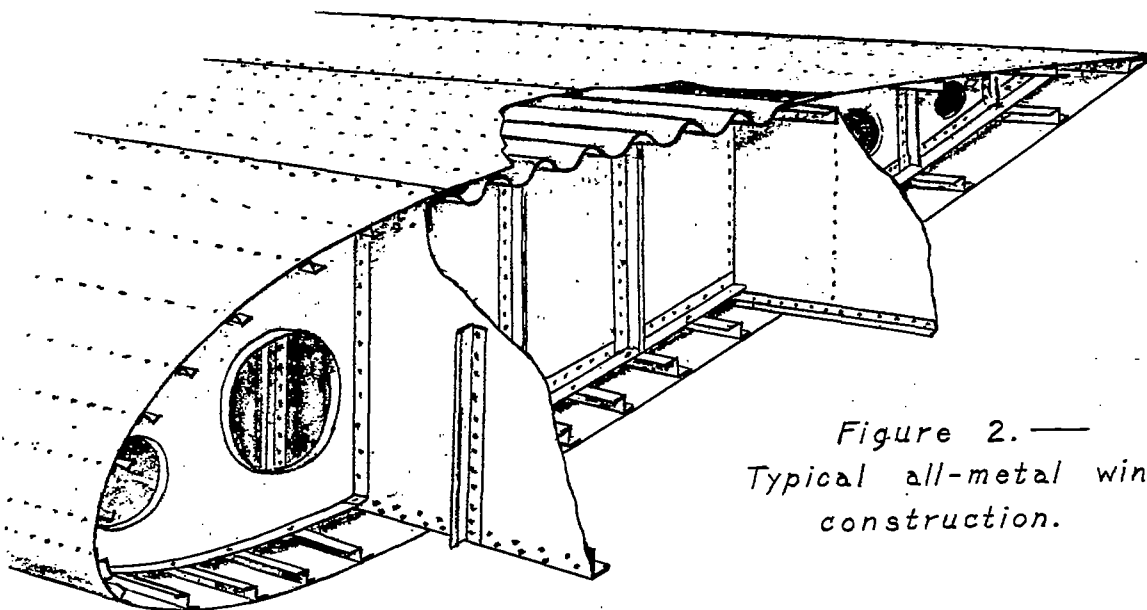


Figure 2. —
Typical all-metal wing
construction.

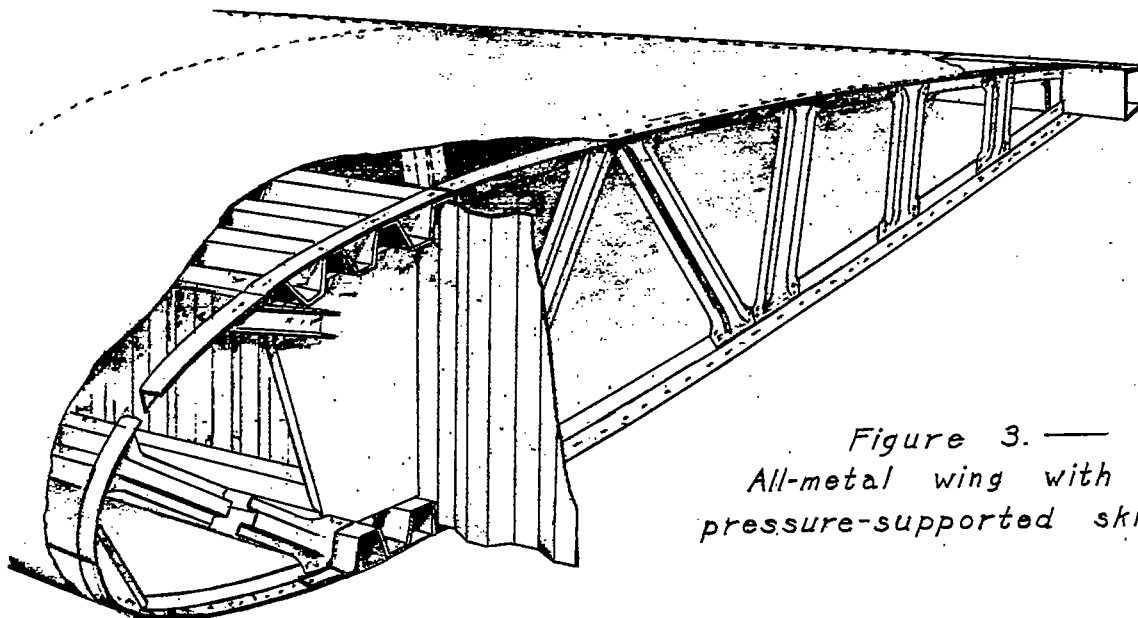


Figure 3. —
All-metal wing with
pressure-supported skin.

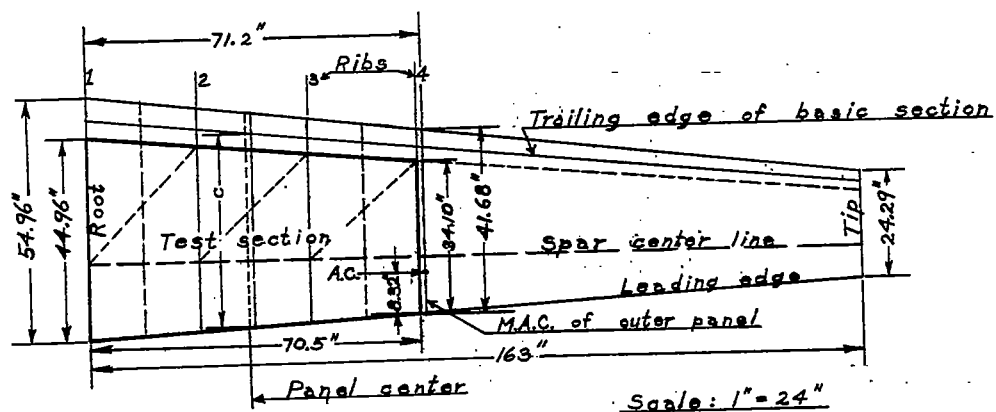


Figure 4. — Plan of outer wing panel.
(At panel center, c = basic chord = 44.00 inches.)

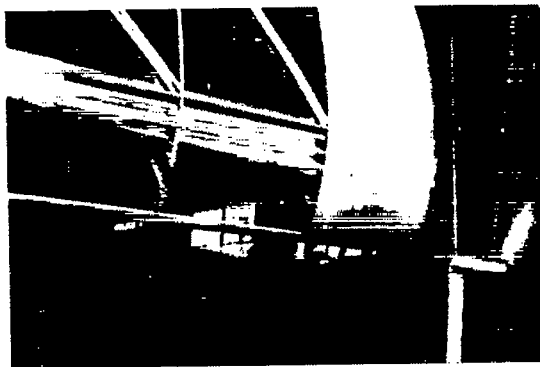


Figure 5.- View showing the internal structure of the wing.



Figure 9.- Bottom surface of wing under half-limit load of condition III with zero pressure, showing tension wrinkles.

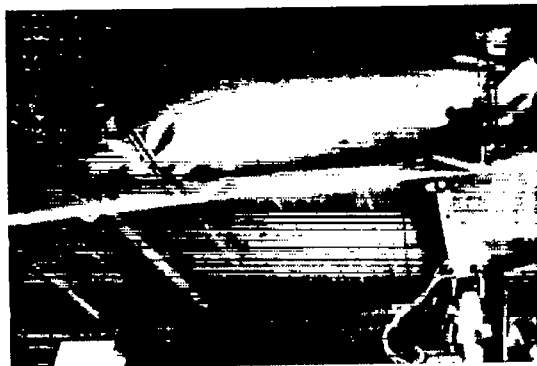


Figure 11.- Top skin bulge under limit load of CAA condition III with zero internal pressure.



Figure 12.- Top skin bulge under limit load of CAA condition III with full dynamic pressure.



Figure 13.- Top surface of wing under half-limit load of condition III with zero internal pressure.



Figure 14.- Top surface of wing after beam failure under a combination of water and shot loading.

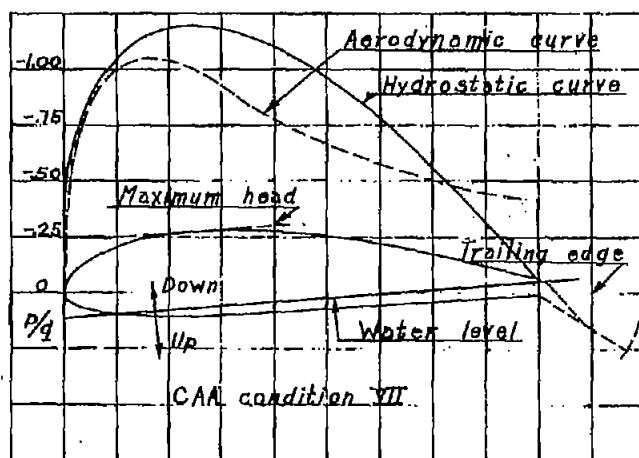
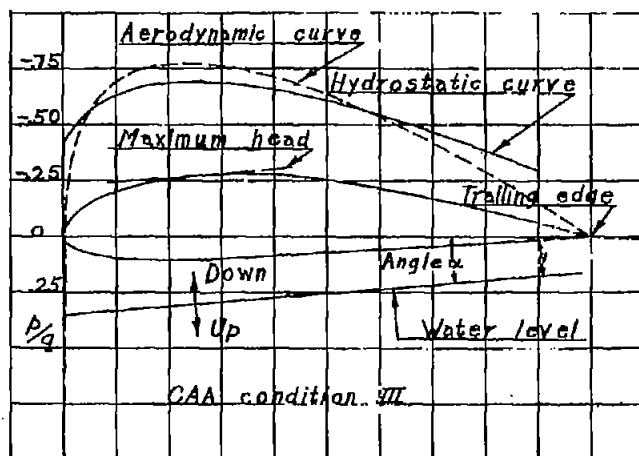


Figure 8.— Hydrostatic and approximate aerodynamic normal pressure curves for top surface (inverted) airfoil section at panel center.

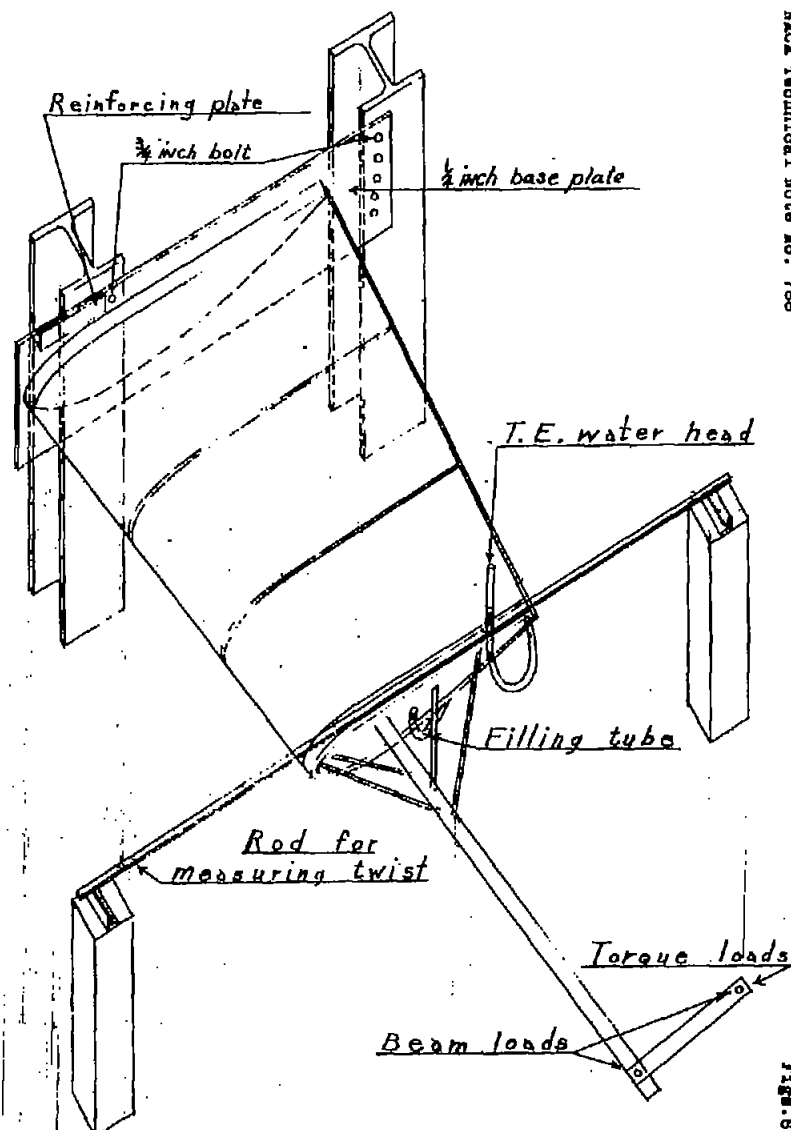


Figure 6.— Arrangement of apparatus for hydrostatic test.

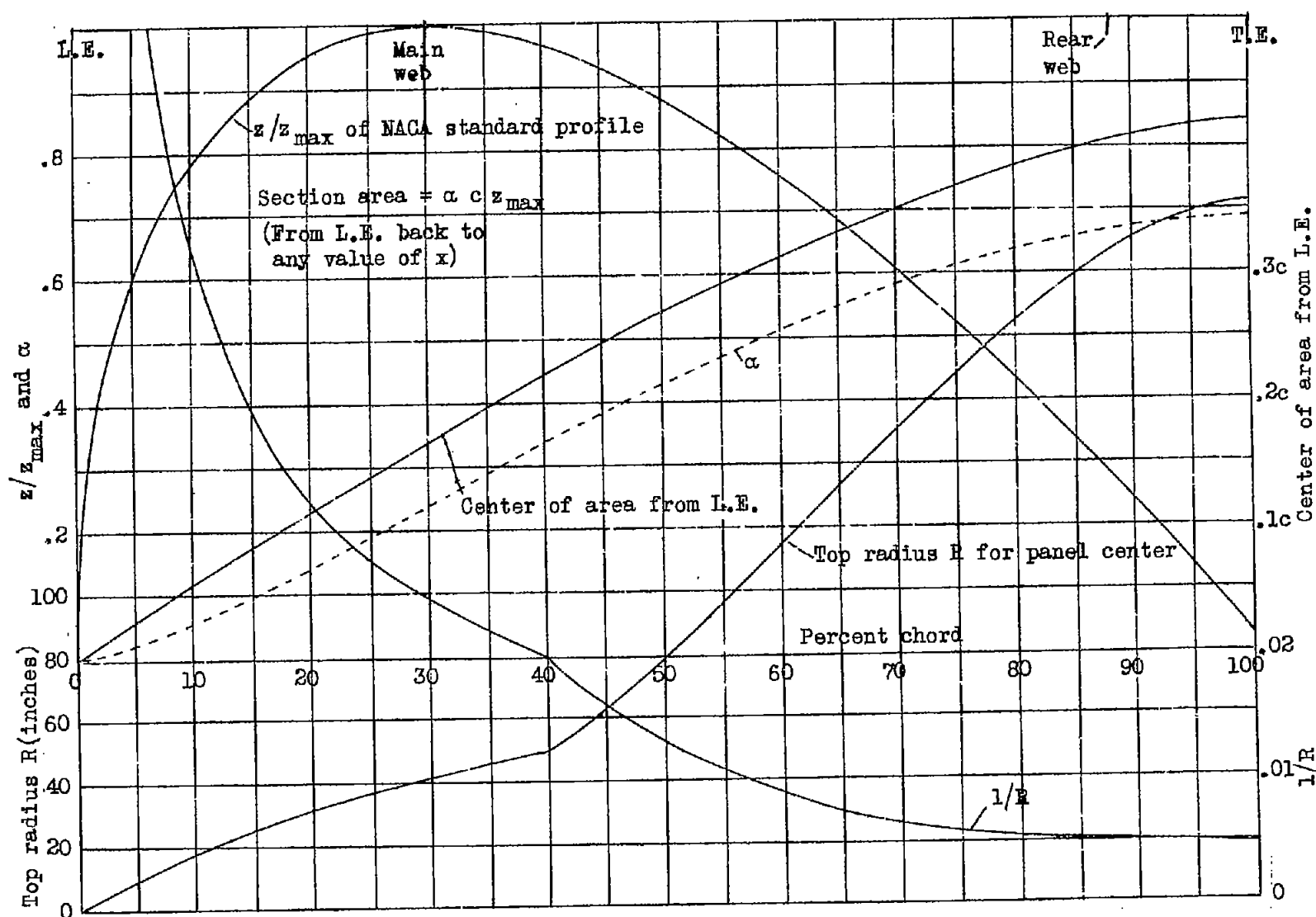


Figure 7.- Geometrical characteristics of wing section.

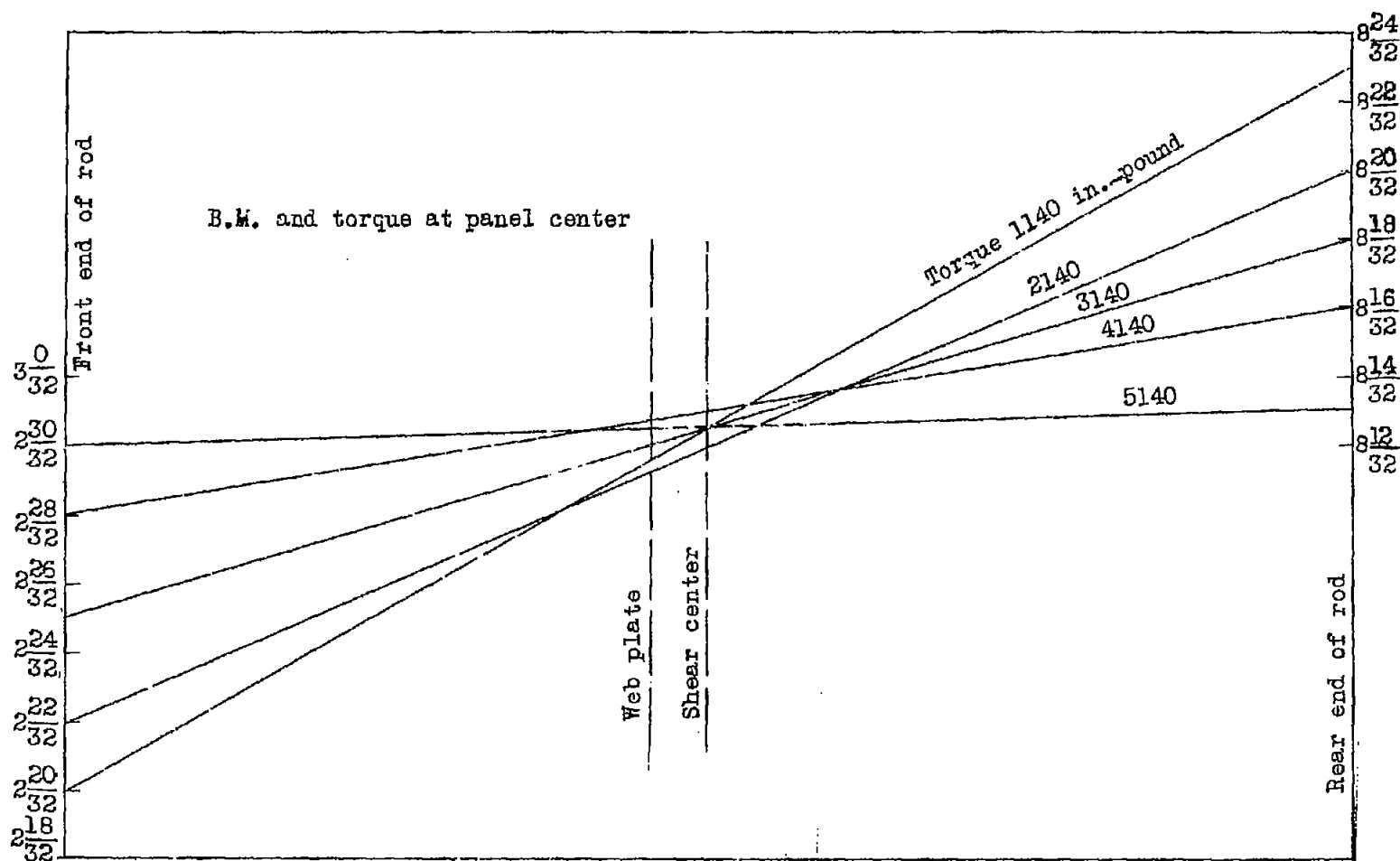


Figure 10.- Plot of position of rod across tip of panel. Shear center taken at average position of rod intersection. CAA condition III. α , 0.078 radians; H, 3.0 inches water; bending moment, 52,300 in.-pounds.